Available online at www.sciencedirect.com
ScienceDirect
International Journal of Heat and Mass Transfer 51 (2008) 993–1002
International Journal of HEAT and MASS TRANSFER
www.elsevier.com/locate/ijhmt

Inverse problem of unsteady conjugated forced convection in parallel plate channels

David T.W. Lin [a], Wei-Mon Yan [b,*], Hung-Yi Li [b]

[a] Department of Mechanical Engineering, Far East University, Hsin-Shih, Tainan County 744, Taiwan, ROC
[b] Department of Mechatronic Engineering, Huafan University, Shih Ting, Taipei 223, Taiwan, ROC

Received 22 December 2006; received in revised form 25 May 2007
Available online 8 August 2007

Abstract

The heat transfer phenomena of the unsteady laminar forced convection in parallel plate channels with wall conduction effects are still not very well understood. An inverse algorithm based on the conjugate gradient method is proposed to estimate the boundary conditions of these problems, and the minimization of object function is used to reduce the estimated error. The estimation of applied heat flux is found to be highly dependent of temperature sensor location and uncertainty, plate thickness, and heating way. The results show that the predicted boundary conditions by the present inverse method are consistent with the initially specified ones.

1. Introduction

In the inverse heat conduction problems, the surface conditions or the thermal properties of a material are estimated by utilizing the temperature measurements within the medium. These problems have received much attention and numerous papers have been devoted to this topic of research. Inverse radiation problems have also been investigated extensively. They are concerned with the determination of the radiative properties or the internal temperature profile of a medium from the measured radiation data. The inverse problems are known as ill-posed, hence the estimation is very sensitive to the measurement errors of the input data. To overcome the instability of the inverse problem, different methods have been developed. Several texts are related to this topic [1–4].

Moutsoglou [5] investigated the steady-state inverse forced convection problem between parallel flat plates. The wall heat flux of the top wall was estimated from measured temperature data at the bottom wall using the straight inversion and the whole domain regularization schemes. Colaco and Orlande [6] investigated the inverse force convection problem to predict two boundary heat fluxes in irregularly shaped channels. Huang and Ozisik [7] determined the spacewise variation of the wall heat flux for laminar flow in a parallel plate duct from temperature measurements inside the flow at several different locations along the flow. Liu and Ozisik [8] estimated the timewise variation of the wall heat flux for transient turbulent forced convection inside parallel plate ducts. The conjugate gradient method with an adjoint equation was adopted to solve the problem. Raghunath [9], Bokar and Ozisik [10], and Liu and Ozisik [11] considered the inverse convection problem of determining the inlet temperature of a thermally developing hydrodynamically developed laminar flow between parallel plates from temperature measurements taken downstream of the entrance. Machado and Orlande [12] applied the conjugate gradient method with an adjoint equation to estimate the timewise and spacewise variation of the wall heat flux in laminar forced convection. Park and Lee [13] employed the Karhunen–Loeve Galerkin procedure to solve the inverse problem of determining the space-dependent wall heat flux for laminar flow inside a duct from the temperature measurement within the flow. Fic [14] studied the steady-state inverse problem to

* Corresponding author. Tel.: +886 2 26632102; fax: +886 2 26633234.
E-mail address: wmyan@cc.hfu.edu.tw (W.-M. Yan).

0017-9310/$ - see front matter © 2007 Elsevier Ltd. All rights reserved.
doi:10.1016/j.ijheatmasstransfer.2007.05.022

Nomenclature

A	dimensionless thermal diffusivity
b	channel width
d	direction of descent
f	the estimated result with measurement errors
f_0	the exact result
J	objective function
K	dimensionless thermal conductivity
k	thermal conductivity
M	the number of the measured data in the X direction
N	the number of the measured data in the τ direction
n_t	the number of the temporal steps
Pe	Pelect number
Q	dimensionless wall heat flux
q	wall heat flux
q_{ref}	reference heat flux
Re	Reynolds number
T	temperature
T_0	initial temperature
t	time
U	dimensionless velocity
u_0	inlet velocity
u	velocity
$\bar{u}$	mean velocity
X, Y	dimensionless coordinates
x, y	coordinates
Y_1	Y coordinate of the sensors
Z	measured dimensionless temperature data

Greek symbols

α	thermal diffusivity
β	step size
δ	plate thickness
ε	the absolute average error
γ	conjugate coefficient
φ	specified positive number
λ	dimensionless plate thickness
ν	kinematic viscosity
θ	dimensionless temperature
σ	standard deviation
τ	dimensionless time
ξ	dimensionless axial coordinate
ζ	random variable

Superscripts

p	pth iteration

Subscripts

f	fluid
w	wall

estimate the boundary velocity. Recently, the present authors considered the estimation of the space and time dependent wall heat flux for unsteady forced convection in a parallel plate duct [15,16] or annular duct [17,18].

It is noted from the paper review cited above, despite its practical importance, that studies of inverse problem of unsteady forced convection in parallel channels with wall conduction effects has not received sufficient attention. This motivates the present investigation. In present work, an attempt is made to examine the estimation of the space and time dependent wall heat flux for unsteady laminar conjugated forced convection between parallel flat plates from the temperature measurements taken at the interface between the fluid and the wall.

2. Analysis

2.1. Direct problem

Consider unsteady laminar forced convection heat transfer in a parallel plate duct with channel width b and plate thickness δ. The flow enters the channel with a fully-developed velocity distribution $u(y)$ and a constant temperature T_0. Initially, the duct walls are kept thermally insulated. At time $t = 0$, the thermal condition of the upper wall at $y = b + \delta$ is suddenly changed and is subjected to wall heating condition with a function of position x and time t. The flow is assumed to have constant properties and the buoyancy term is neglected. It is intended to provide a first step toward future work, which these effects will be considered. Fig. 1 describes the geometry and coordinates. By introducing the following dimensionless quantities

$$X = \frac{x}{bPe}, \quad Y = \frac{y}{b}, \quad \tau = \frac{\alpha_f t}{b^2}, \quad \theta = \frac{k(T - T_0)}{bq_{ref}}$$
$$Pe = \frac{\bar{u}b}{\alpha_f}, \quad U = \frac{u}{\bar{u}}, \quad Q = \frac{q}{q_{ref}}, \quad U = \frac{3}{2}[1 - (2Y - 1)^2]$$
$$K = \frac{k_w}{k_f}, \quad \lambda = \frac{\delta}{b}, \quad A = \frac{\alpha_w}{\alpha_f}, \tag{1}$$

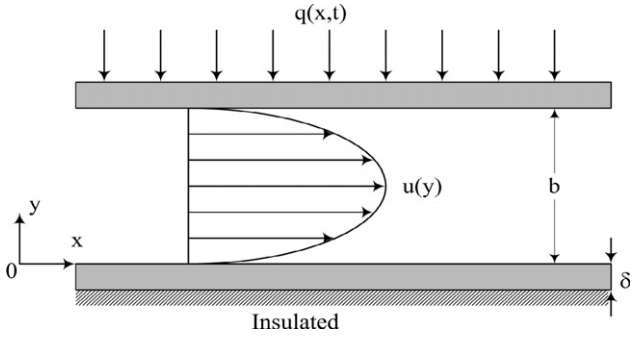

Fig. 1. Geometry and coordinates.

where k_w and k_f is the thermal conductivity of the plate and the fluid, respectively, α_w and α_f is the thermal diffusivity of the plate and fluid, separately, T is the temperature, q is the wall heat flux, q_{ref} is the reference heat flux, and $\bar{u}$ is the mean velocity. In this paper, the heat transfer to the wall is assumed positive.

The governing energy conservation equation based on the dimensionless form inside the fluid and the plate for the problem are given by

$$\text{Fluid} \quad \frac{\partial \theta_f}{\partial \tau} + U\frac{\partial \theta_f}{\partial X} = \frac{\partial^2 \theta_f}{\partial Y^2}, \tag{2a}$$

$$\text{Plate} \quad \frac{\partial \theta_w}{\partial \tau} = A\frac{\partial^2 \theta_w}{\partial Y^2} \tag{2b}$$

with the initial condition and the boundary conditions

$$\theta_f(X,Y,0) = \theta_w(X,Y,0) = 0, \tag{2c}$$

$$\theta_f(0,Y,\tau) = 0, \tag{2d}$$

$$\frac{\partial \theta_w(X,-\lambda,\tau)}{\partial Y} = 0, \tag{2e}$$

$$K\frac{\partial \theta_w(X,0,\tau)}{\partial Y} = \frac{\partial \theta_f(X,0,\tau)}{\partial Y}, \tag{2f}$$

$$K\frac{\partial \theta_w(X,1,\tau)}{\partial Y} = \frac{\partial \theta_f(X,1,\tau)}{\partial Y}, \tag{2g}$$

$$K\frac{\partial \theta_w(X,1+\lambda,\tau)}{\partial Y} = Q(X,\tau). \tag{2h}$$

The direct problem can be solved to obtain the dimensionless temperature field. A fully implicit numerical scheme in which the x-direction convection term is approximated by the upstream difference, the y-direction diffusion term by the central difference and the unsteady term by the backward difference is employed to transform the governing equations into finite difference equations. The detail descriptions about the numerical method are described in [19]. This system of equations forms a tridiagonal matrix which can be solved by the Thomas Algorithm [20].

2.2. Inverse problem

In the direct problem, the velocity distribution, the initial condition, and the boundary conditions are given to determine the temperature distribution in the flow field and the plate. In the inverse problem, the temperature data are assumed to be measured inside the flow or at the interface between fluid and wall. The dimensionless heat flux at the upper wall, $Q(X,\tau)$, is recovered by using the measured data. The estimation of the wall heat flux from the knowledge of the measured temperature data can be constructed as a problem of minimization of the objective function

$$J = \sum_{i=1}^{M}\sum_{k=1}^{N}(\theta_{f,i,k} - Z_{i,k})^2, \tag{3}$$

where $\theta_{f,i,k} = \theta_f(X_i, Y_1, \tau_k)$ is the calculated dimensionless temperature for an estimated $Q(X,\tau)$, $Z_{i,k} = Z(X_i, Y_1, \tau_k)$ is the measured dimensionless temperature. If $Y_1 = 0$, the measurements are taken at the lower interface between the fluid and the wall; if $0 < Y_1 < 1$, the measurements are taken inside the fluid; if $Y_1 = 1$, the measurements are taken at the upper interface between the fluid and the wall. M and N are the numbers of the measured points in the X and τ directions, respectively.

In this paper, the conjugate gradient method [21] is employed to determine the unknown wall heat flux $Q(X,\tau)$ by minimizing the objective function, J. The iterative process is

$$Q^{p+1}_{m,n} = Q^p_{m,n} - \beta^p d^p_{m,n}, \tag{4}$$

where $Q_{m,n} = Q(X_m, \tau_n)$, β^p is the step size, $d^p_{m,n}$ is the direction of descent which is determined from

$$d^p_{m,n} = \left(\frac{\partial J}{\partial Q_{m,n}}\right)^p + \gamma^p d^{p-1}_{m,n} \tag{5}$$

and the conjugate coefficient γ^p is computed from

$$\gamma^p = \frac{\sum_{m=1}^{M}\sum_{n=1}^{N}\left[\left(\frac{\partial J}{\partial Q_{m,n}}\right)^p\right]^2}{\sum_{m=1}^{M}\sum_{n=1}^{N}\left[\left(\frac{\partial J}{\partial Q_{m,n}}\right)^{p-1}\right]^2} \quad \text{with } \gamma^0 = 0. \tag{6}$$

Here, $\frac{\partial J}{\partial Q_{m,n}}$ is the gradient of the objective function. The step size is determined from

$$\beta^p = \frac{\sum_{i=1}^{M}\sum_{k=1}^{N}\left(\theta^p_{f,i,k} - Z_{i,k}\right)\sum_{m=1}^{M}\sum_{n=1}^{N}\left(\frac{\partial \theta_{f,i,k}}{\partial Q_{m,n}}\right)^p d^p_{m,n}}{\sum_{i=1}^{M}\sum_{k=1}^{N}\left[\sum_{m=1}^{M}\sum_{n=1}^{N}\left(\frac{\partial \theta_{f,i,k}}{\partial Q_{m,n}}\right)^p d^p_{m,n}\right]^2}, \tag{7}$$

where $\frac{\partial \theta_{f,i,k}}{\partial Q_{m,n}}$ is the sensitivity coefficient. To calculate the sensitivity coefficient, the direct problem is differentiated with respect to $Q_{m,n}$ to obtain the sensitivity problem, i.e.,

$$\frac{\partial}{\partial \tau}\left(\frac{\partial \theta_f}{\partial Q_{m,n}}\right) + U\frac{\partial}{\partial X}\left(\frac{\partial \theta_f}{\partial Q_{m,n}}\right) = \frac{\partial^2}{\partial Y^2}\left(\frac{\partial \theta_f}{\partial Q_{m,n}}\right), \tag{8a}$$

$$\frac{\partial}{\partial \tau}\left(\frac{\partial \theta_w}{\partial Q_{m,n}}\right) = A\frac{\partial^2}{\partial Y^2}\left(\frac{\partial \theta_w}{\partial Q_{m,n}}\right), \tag{8b}$$

$$\frac{\partial \theta_f(X,Y,0)}{\partial Q_{m,n}} = \frac{\partial \theta_w(X,Y,0)}{\partial Q_{m,n}} = 0, \tag{8c}$$

$$\frac{\partial \theta_f(0,Y,\tau)}{\partial Q_{m,n}} = 0, \tag{8d}$$

$$\frac{\partial}{\partial Y}\left(\frac{\partial \theta_w(X,-\lambda,\tau)}{\partial Q_{m,n}}\right) = 0, \tag{8e}$$

$$K\frac{\partial}{\partial Y}\left(\frac{\partial \theta_w(X,0,\tau)}{\partial Q_{m,n}}\right) = \frac{\partial}{\partial Y}\left(\frac{\partial \theta_f(X,0,\tau)}{\partial Q_{m,n}}\right), \tag{8f}$$

$$K\frac{\partial}{\partial Y}\left(\frac{\partial \theta_w(X,1,\tau)}{\partial Q_{m,n}}\right) = \frac{\partial}{\partial Y}\left(\frac{\partial \theta_f(X,1,\tau)}{\partial Q_{m,n}}\right), \tag{8g}$$

$$K\frac{\partial}{\partial Y}\left(\frac{\partial \theta_w(X,1+\lambda,\tau)}{\partial Q_{m,n}}\right) = \hat{u}(X - X_m, \tau - \tau_n) \tag{8h}$$

for $m = 1, 2, \ldots, M; n = 1, 2, \ldots, N$, where

$$\hat{u}(X - X_m, \tau - \tau_n) = \begin{cases} 1 & \text{if } X = X_m, \quad \tau = \tau_n, \\ 0 & \text{otherwise.} \end{cases} \tag{8f}$$

The gradient of the objective function, $\frac{\partial J}{\partial Q_{m,n}}$, is determined by differentiating Eq. (3) with respect to $Q_{m,n}$ to obtain

$$\frac{\partial J}{\partial Q_{m,n}} = 2 \sum_{i=1}^{M} \sum_{k=1}^{N} (\theta_{i,k} - Z_{i,k}) \frac{\partial \theta_{f,i,k}}{\partial Q_{m,n}}. \tag{9}$$

If the problem contains no measurement errors, the condition

$$J(Q^p_{m,n}) < \varphi, \tag{10}$$

can be used for terminating the iterative process, where φ is a small specified positive number. However, the measured temperature data contain measurement errors. Following the computational experience, we use the discrepancy principle [22]

$$J(Q^p_{m,n}) < MN\sigma^2 \tag{11}$$

as the stopping criterion, where σ is the standard deviation of the measurement errors.

The computational procedure for the solution of the inverse convection problem is summarized as follows:

Step 1: Solve the sensitivity problem to calculate the sensitivity coefficient $\frac{\partial \theta_{f,i,k}}{\partial Q_{m,n}}$. Step 2: Pick an initial guess $Q^0_{m,n}$. Set $p = 0$. Step 3: Solve the direct problem to compute $\theta_{f,i,k}$. Step 4: Calculate the objective function. Terminate the iteration process if the specified stopping criterion is satisfied. Otherwise go to Step 5. Step 5: Knowing $\frac{\partial \theta_{f,i,k}}{\partial Q_{m,n}}$, $\theta_{f,i,k}$, and $Z_{i,k}$, compute the gradient of the objective function $\frac{\partial J}{\partial Q_{m,n}}$. Step 6: Knowing $\frac{\partial J}{\partial Q_{m,n}}$, compute γ^p and $d^p_{m,n}$. Step 7: Knowing $\frac{\partial \theta_{f,i,k}}{\partial Q_{m,n}}$, $\theta_{f,i,k}$, $Z_{i,k}$, and $d^p_{m,n}$, compute β^p. Step 8: Knowing β^p and $d^p_{m,n}$, compute $Q^{p+1}_{m,n}$. Set $p = p + 1$ and go to Step 3. In this paper, the initial guess is assumed as zero.

3. Results and discussion

To demonstrate the accuracy of the proposed method for the estimation of the upper wall heat flux from the simulated measured temperature data, the effects of the measurement error, the sensor location, and the plate thickness on the results of the inverse analysis are investigated. In the present study, three kinds of boundaries (i.e., the interface between the plate and the fluid, the quantity of the heat flux entering the top plate surface, and the adiabatic boundary in the bottom plate) are applied on the parallel plate channel as shown in Fig. 1.

The measured temperature data, Z, are simulated by adding random errors to the exact temperature, θ, computed from the solution of the direct problem

$$Z = \theta + \sigma\zeta, \tag{12}$$

where σ is the standard deviation of the measurement data, ζ is a random variable of normal distribution with zero mean and unit standard deviation. The value of ζ is calculated by the IMSL subroutine DRNNOR [23] and chosen over the range $-2.576 < \zeta < 2.576$, which represent the 99% confidence bound for the measured temperature.

In this work, the unknown wall heat fluxes are assumed to be three different kinds of function to examine the accuracy of the estimated results, separately. These wall heat fluxes are listed as below

$$\text{Case 1:} \quad Q(\tau) = 20\tau, \quad \tau \leqslant 0.5, \tag{13a}$$

$$Q(\tau) = 20(1 - \tau), \quad \tau > 0.5, \tag{13b}$$

$$\text{Case 2:} \quad Q(\tau) = 20\sin(\pi\tau), \tag{13c}$$

$$\text{Case 3:} \quad Q(X, \tau) = 20X\sin(\pi\tau). \tag{13d}$$

The heat fluxes of cases 1 and 2 are the time dependent triangular and sinusoidal functions, separately. While, the case 3 is the space and time dependent wall heat flux. In this work, the inverse solutions for the temperature measurements taken inside the fluid or at the interface between the fluid and the wall are investigated. Additionally, the accuracy of the estimated heat fluxes are discussed with different plate thickness, measurement errors and sensor locations. The dimensionless thickness of the plate, λ, is assumed as 0.0, 0.05, 0.1, and 0.2, respectively. In addition, forty-one equally spaced measurements are taken both in $0 \leqslant X \leqslant 1$ and $0 \leqslant \tau \leqslant 1$ for all the cases considered. The data are used as input to reconstruct the unknown wall heat flux in the inverse problem. Typical properties are applied as $k_w = 17.0$ W/mK, $\alpha_w = 4.4 \times 10^{-6}$ m^2/s (stainless steel); and $k_f = 0.6$ W/mK, $\alpha_f = 1.5 \times 10^{-7}$ m^2/s (water). It is initially at an uniform temperature $T_0 = 0$ °C.

To investigate the deviation of the estimated results from the error-free solution, the absolute average errors for the estimated solutions are defined as follows

$$\varepsilon = \frac{1}{n_t} \sum_{j=1}^{n_t} |f - f_0|, \tag{14}$$

where the f is the estimated result with measurement errors and the f_0 is the exact result. n_t is the number of the temporal steps. It is clear that a smaller value of ε indicates a better estimation and vice versa.

Effects of wall thickness of channel plate on the predicted wall heat fluxes are presented in Fig. 2. In this figure, the wall heat flux of case 1 is applied on the top plate. Besides, the sensor location is selected to be $Y_1 = 0.9$ and the measurement error, σ, is 0.03 or 0.06. These profiles of the estimated heat flux are compared to the exact heat flux in order to investigate the deviation between the estimated and exact results. It is clear from Fig. 2 that the estimated wall heat flux coincides with the exact input data, i.e., $\sigma = 0.0$. In addition, the accuracy of the inverse analysis is also good for the simulated experimental data containing errors of standard deviation $\sigma = 0.03$ and $\sigma = 0.06$ at the dimensionless plate thickness, $\lambda = 0.2$. The absolute average errors of the estimated dimensionless heat flux are, respectively, to be appropriately 0.071 and

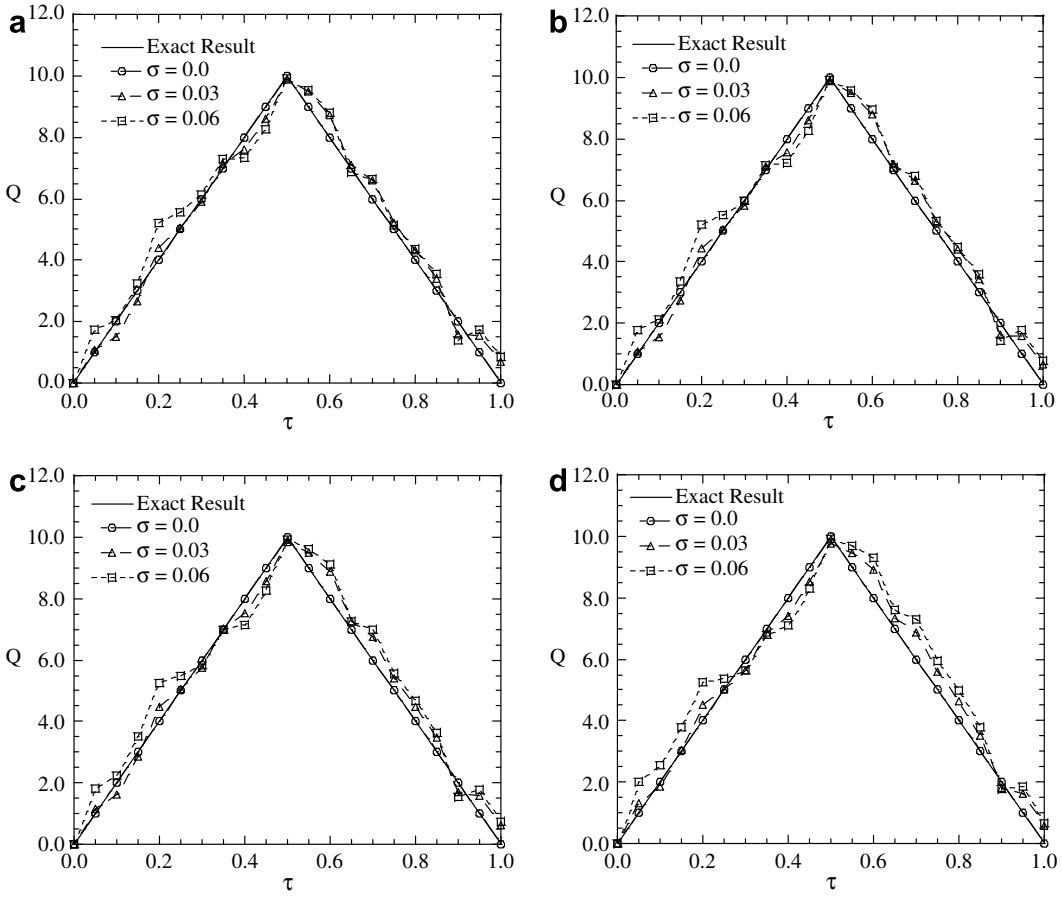

Fig. 2. Estimation of the wall heat flux by inverse analysis for wall heating condition of case 1 under different wall thickness. (a) $\lambda = 0.0$; (b) $\lambda = 0.05$; (c) $\lambda = 0.1$ and (d) $\lambda = 0.2$.

0.098 for $\sigma = 0.03$ and $\sigma = 0.06$. A close examination of Fig. 2a–d discloses that the deviations between the estimated and exact results are slightly affected by the plate thickness, λ.

To illustrate the effects of measurement error and wall thickness on the absolute average error, Fig. 3 presents the distributions of the absolute average errors under various conditions which the σ ranges from 0.0 to 0.09 and the λ is 0.0, 0.05, 0.1 and 0.2, separately. In general, large measuring errors make the estimated results to diverge from the error-free solutions. It is clear in Fig. 3 that the absolute average error decreases with a decrease in the measurement error. Additionally, the absolute average error increases slightly with the dimensionless plate thickness. From the results mentioned above, it can be concluded that the proposed method is accurate and stable to estimate the transient heat flux in the conjugated forced convection problem. For the tabulated forms allow the facts to be read clearly, the absolute average errors of the estimated results in Fig. 3 are shown in Table 1. It is noted in Table 1 that the absolute average errors are relatively amplified when the σ is increased from 0.03 to 0.06, compared to that when σ is changed from 0.06 to 0.09. It is also found that the more inaccurate estimated results are noted for the channel with a thicker wall.

The sensor location in the y-direction is an important parameter affecting the estimated results in the inverse problem. To examine the effects of the sensor location on the estimated wall heat flux, Fig. 4 shows the estimated and exact results at different sensor locations Y_1 (= 0.2, 0.5, and 0.8) for the condition of $\sigma = 0.01$ and $\lambda = 0.2$. A careful inspection of Fig. 4 reveals that the deviations between the estimated and exact results become significant when the Y_1 is decreased. This means that the error of the estimated heat flux is larger as the sensor location is more far from the top plate. This is in agreement with the general concept in the inverse analysis that the more far away the unknown wall heat flux the sensors are, the more inaccurate the estimation is. In addition, the absolute average error is about 0.137 as $Y_1 = 0.0$, $\sigma = 0.09$ and $\lambda = 0.2$. The corresponding relative error is about 1.37%, where the relative error is defined as the absolute average error divided by the maximum wall heat flux. This confirms that in the present study, the proposed method is excellent even the estimated conditions are strict.

According to the description of Fig. 4, the relationship among the absolute average error, the measurement error and the sensor location is also interesting in the inverse problem. Fig. 5 presents the distributions of the absolute average error for various conditions of the absolute

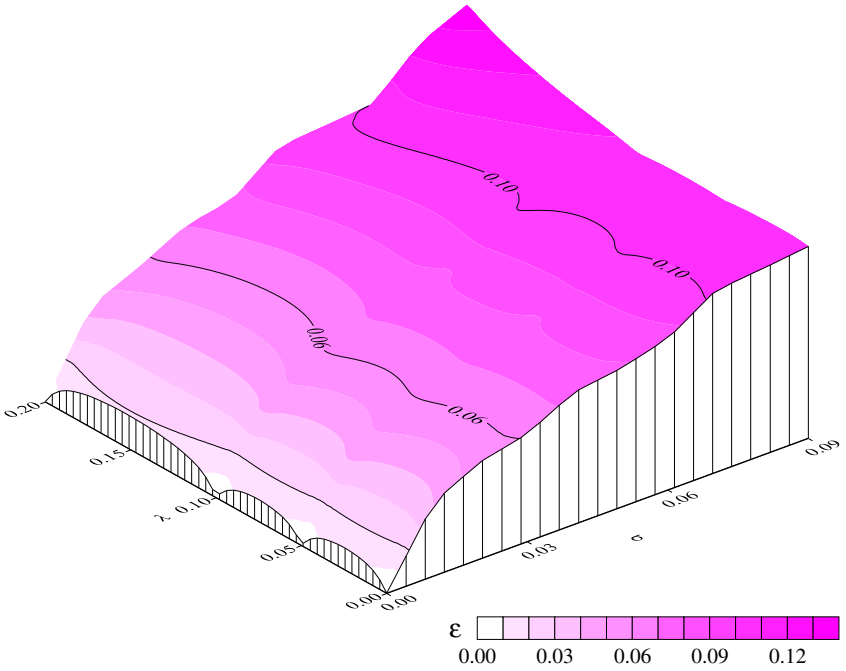

Fig. 3. The contours of the absolute average error of the estimated heat flux for different measurement errors and plate thickness for wall heating condition of case 1.

Table 1
The absolute average errors at different σ and λ for wall heating condition of case 1

	$\sigma = 0.03$	$\sigma = 0.06$	$\sigma = 0.09$
$\lambda = 0.0$	0.061	0.086	0.109
$\lambda = 0.05$	0.066	0.093	0.108
$\lambda = 0.1$	0.069	0.099	0.107
$\lambda = 0.2$	0.071	0.098	0.137

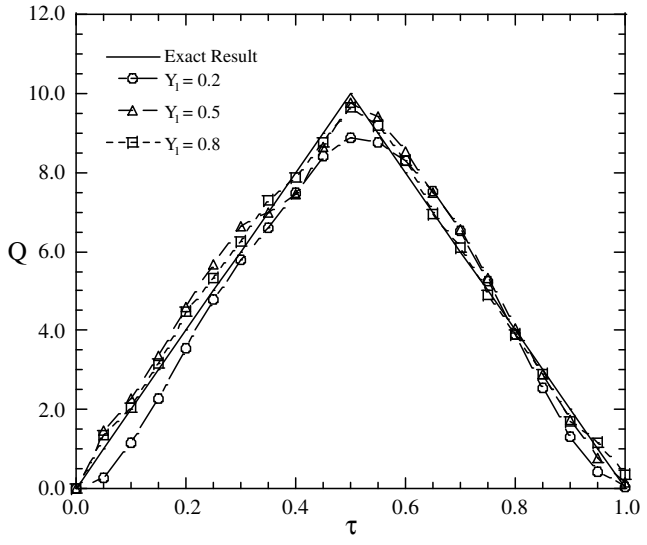

Fig. 4. Estimation of the wall heat flux by inverse analysis for wall heating condition of case 1 ($\sigma = 0.01$, $\lambda = 0.2$).

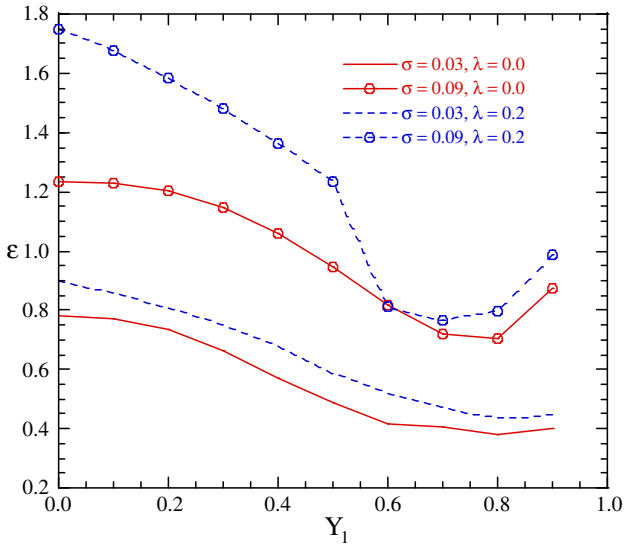

Fig. 5. Effects of sensor location on the absolute average error of the estimated heat flux for wall heating condition of case 1 ($\sigma = 0.01$, $\lambda = 0.0$).

average error, the measurement error and the sensor location. It is clearly observed from Fig. 5 that the absolute average error is rapidly reduced when Y_1 is raised from 0.2 to 0.6. But, the absolute average error does not decay with an increase in Y_1 when Y_1 is closer to the top plate ($Y_1 > 0.8$). In addition, the absolute average error is about 0.175, even the sensor location is located at $Y_1 = 0.0$ with measurement error σ being 0.09. In general, despite the value of σ, a better estimation appears when the sensor location is closer to the unknown wall heat flux boundary. Namely, an accurate value of estimated heat flux could result either from a low value of the measurement error, which would indicate a better convergence in the present

proposed method, or from a sensor location nearer the heat flux boundary. Moreover, we notice that the estimated result is more accurate as the plate is thinner regardless of σ and Y_1.

To further test the applicability of the proposed method, the same measured conditions as previous wall heat flux conditions (case 1) are adopted to estimate the unknown wall heat flux with cases 2 and 3. Therefore, the applied wall heat flux is changed to be case 2. The effects of the plate thickness, the measurement error and the sensor location are investigated again. This clarifies that the proposed method is suitable to deal with the different forms of wall heat flux. The estimated heat fluxes resulted from the different measurement error and plate thickness are shown in Fig. 6a–d and compared with the exact heat flux. Overall inspection of Fig. 6a–d and the comparison of Figs. 2 and 6 disclose that the similar trend is found. The accurate estimated result is noted for a case with a small measurement error.

The contours of the absolute average error related to the measurement error, the dimensionless plate thickness and the sensor location are presented in Figs. 7 and 8. To illustrate the absolute average errors are presented in Fig. 7 at different measurement error and dimensionless plate thickness. In Fig. 7, as expected, the accuracy of the estimation is much better for the cases with lower measurement error and thinner wall thickness. The effects of the sensor location on the accuracy for wall heat condition of case 2 are presented in Fig. 8. It is observed from Fig. 8 that the effect of the sensor location has the same trend with the wall heating condition of case 1 (see Fig. 5). When the measurements are inside the fluid, i.e., $Y_1 = 0.9$, the agreement between the estimated and the exact values of the wall heat flux is good as the case 1. The result is also satisfactory when the measured data are taken at the lower wall, i.e., $Y_1 = 0$. However, from the experimental point of view, it is desirable to avoid sensors within the fluid which will disturb the flow field and introduce errors.

Finally, the wall heating condition of case 3 which is a function of space (X) and time (τ) is tested. Fig. 9 presents the contours of the average absolute error. It is found in Fig. 9 that like the other wall heating conditions, the effects of the measurement error and plate thickness on the absolute average error is similar. Therefore, it can be concluded that the accuracy of the estimated result is dominated by the measurement error. While the influences of wall thickness or unknown wall heating conditions on the accuracy of the estimated result are slightly. It is found in

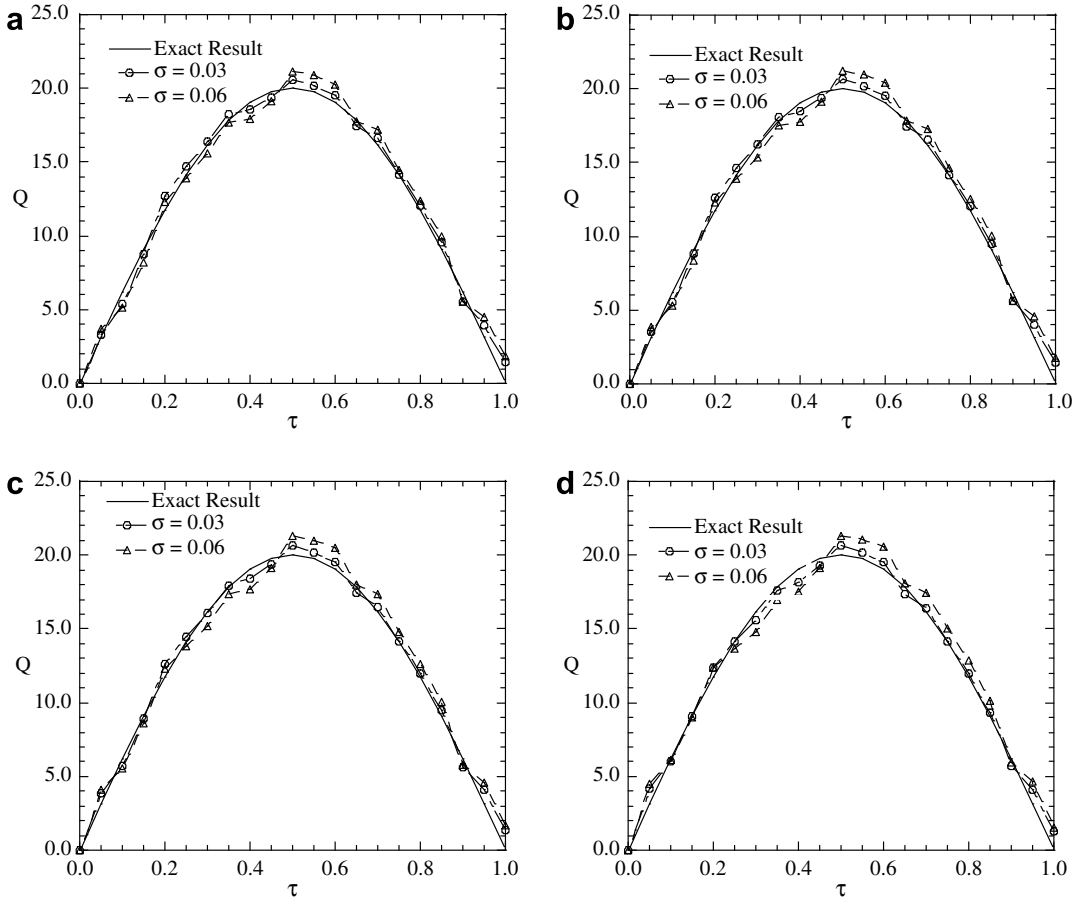

Fig. 6. Estimation of the wall heat flux by inverse analysis for wall heating condition of case 2 under different wall thickness. (a) $\lambda = 0.0$; (b) $\lambda = 0.05$; (c) $\lambda = 0.1$ and (d) $\lambda = 0.2$ ($Y_1 = 0$).

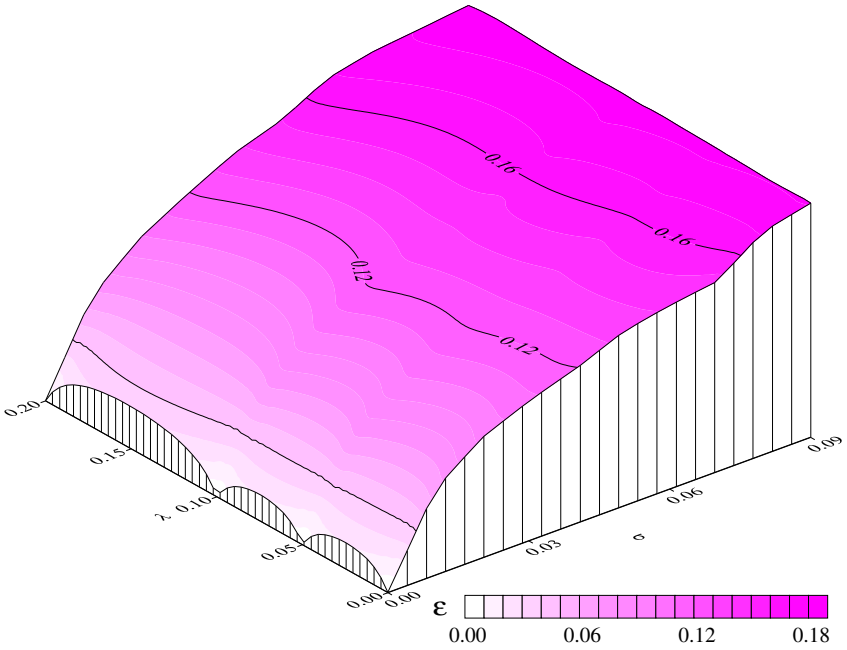

Fig. 7. The contours of absolute average error of the estimated heat flux for different measurement errors and plate thickness for wall heating condition of case 2.

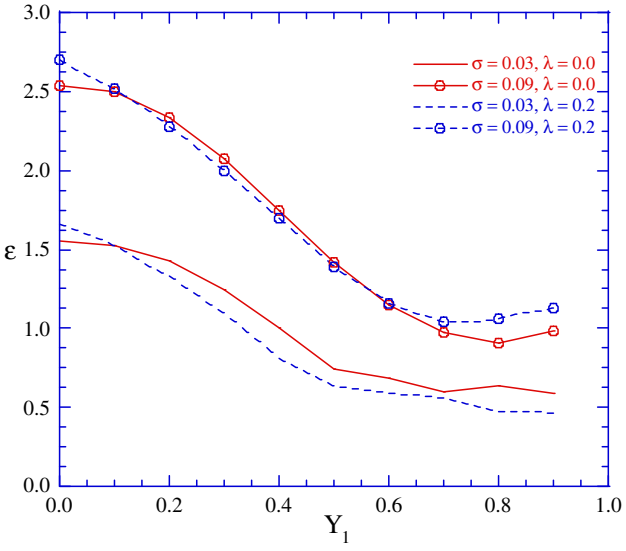

Fig. 8. Effects of sensor locations on the absolute average error of the estimated heat flux for wall heating condition of case 2 ($\sigma = 0.01$, $\lambda = 0.0$).

the separate numerical runs that the absolute average error is 0.137, 0.185 and 0.171 at $\sigma = 0.09$ and $\lambda = 0.2$ for wall heating conditions of cases 1–3 separately. The corresponding relative errors are about 1.37%, 0.93%, and 0.85% as the error of the measured temperature is about 0.5 °C.

It is also interesting to investigate the effect of the sensor locations on the estimated results. Fig. 10 shows the estimated heat fluxes at $X = 0.3$, 0.6, 0.9 under different sensor locations ($Y_1 = 0.2$, 0.5, and 0.8) for wall heating conditions of case 3. A careful examination of Fig. 10 indicates that a larger deviation between the estimated and exact results is noted for a larger X ($= 0.9$). Besides, the value of the estimated result increases with an increase in the location X. The reason is that the heat flux is dependent on X and accumulates its value as X increases. The effects of sensor location Y_1 can be found in this figure. Like Fig. 4, the sensor location is an important parameter that influences the estimation of the heat flux.

The effects of sensor locations on the absolute average errors under different measurement error and wall thickness are presented in Fig. 11. Like the results in wall heating conditions of cases 1 and 2 (Figs. 5 and 8), the estimated heat fluxes are more accurate with sensor location being closer to the top boundary, with the thinner wall or within the thermal boundary layer. The absolute average errors in Fig. 11 are tabulated in Table 2. As is evident from Table 2, the case of lower sensor location or the thicker wall is less accurate than the case of upper sensor location or the thinner wall. For examples, the values of absolute average error at $\lambda = 0.2$ and $\sigma = 0.09$ are 2.34, 1.99, 0.99, and 0.91 when $Y_1 = 0.0$, 0.3, 0.6, and 0.9, respectively. In addition, we observe that the estimated heat fluxes are extremely accurate at $\lambda = 0.0$, 0.2 and $\sigma = 0.0$. These results prove that this present inverse algorithm is reliable in advance. In addition, we found that the reduced ratio (51%) of the variation of the absolute average errors is exhibited as Y_1 is increased from 0.2 to 0.6, where the reduced ratio is defined as $|\varepsilon_{Y_1=0.02} - \varepsilon_{Y_1=0.06}|/\varepsilon_{Y_1=0.06}$. The results show that the values of absolute average error decrease apparently as the sensor location is close to the unknown heat flux boundary for all kinds of wall thickness in spite of the form of heat flux. The above phenomena illustrate the difficulty of the conjugated forced convection

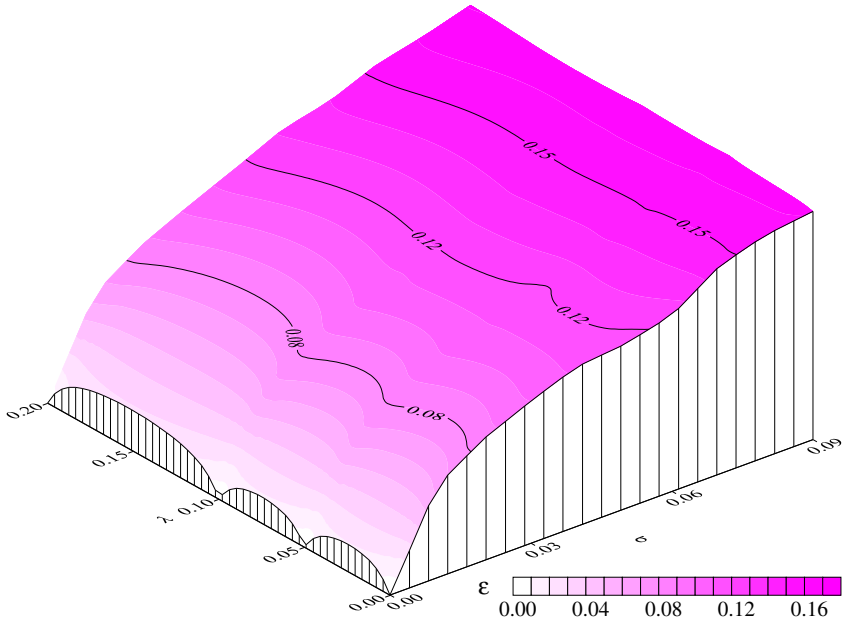

Fig. 9. The contours of the absolute average errors of the estimated heat flux for different measurement errors and plate thickness for wall heating condition of case 3.

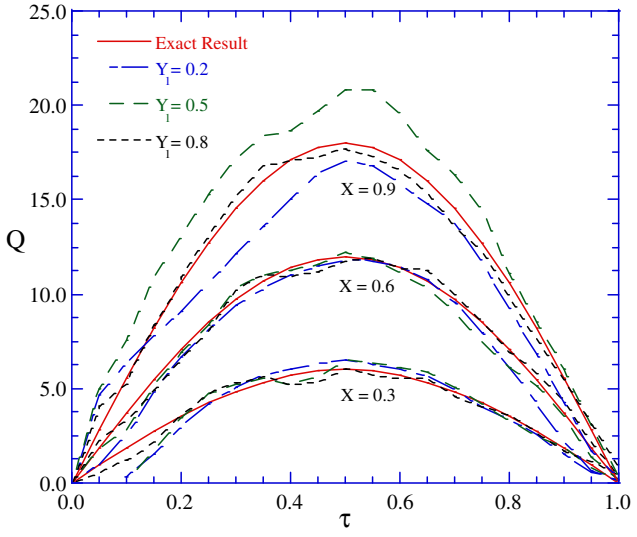

Fig. 10. Effects of the variations of sensor locations on the estimated results for unknown wall heating condition of case 3 for $\sigma = 0.01$ and $\lambda = 0.2$.

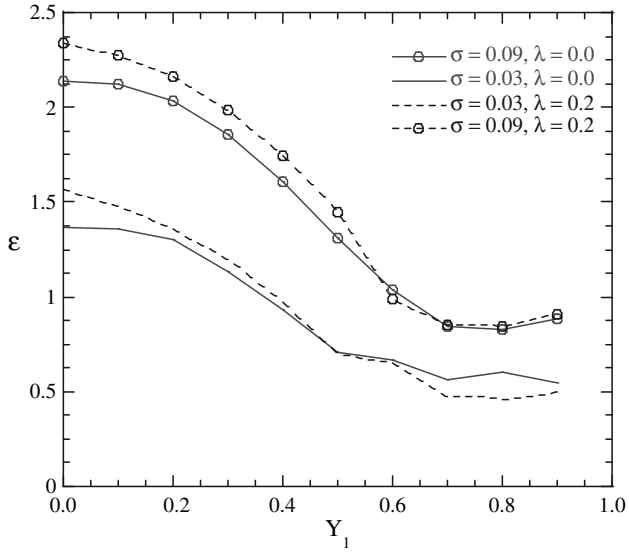

Fig. 11. Effects of sensor locations on the absolute average errors of the estimated heat flux for unknown wall heating condition of case 3.

Table 2
The absolute average errors at different σ and λ for wall heating condition of case 3

Y_1		0.0	0.1	0.2	0.3	0.4	0.5	0.6	0.7	0.8	0.9
$\lambda = 0.2$	$\sigma = 0.0$	0.013	0.01	0.006	0.003	0.0	0.0	0.0	0.0	0.0	0.0
	$\sigma = 0.03$	1.566	1.482	1.361	1.199	0.97	0.698	0.652	0.474	0.46	0.498
	$\sigma = 0.09$	2.341	2.275	2.162	1.988	1.743	1.443	0.986	0.856	0.841	0.91
$\lambda = 0.0$	$\sigma = 0.0$	0.007	0.006	0.004	0.001	0.0	0.0	0.0	0.0	0.0	0.0
	$\sigma = 0.03$	1.369	1.358	1.305	1.135	0.935	0.705	0.67	0.563	0.607	0.546
	$\sigma = 0.09$	2.138	2.12	2.034	1.856	1.606	1.310	1.036	0.847	0.827	0.888

problem clearly when the measurement error, the sensor location and the plate thickness are considered in the inverse analysis.

In this section, the considerations of the different heat flux functions demonstrate the validity of the proposed method. In addition, the larger deviations are appeared when the measurement error is larger. In this paper, lots of cases which include the different plate thickness, the variation of the sensor location, and the different measurement error are exhibited to demonstrate the reliability of this proposed method. Therefore, the proposed method is able to deal with the inverse conjugated forced convection problem accurately.

4. Conclusions

The estimation of the space and time dependent wall heat flux for unsteady conjugated forced convection between parallel flat plates has been considered. The conjugate gradient method is applied to solve the problem. Various types of wall heat fluxes are used to test the accuracy of the method. The inverse solutions are satisfactory for both exact and noisy data. As expected, the results also show that the more far away the unknown wall heat flux the sensors are, the more inaccurate the estimation is. In addition, the more accurate estimated results are appeared in the thinner wall condition in spite of any kinds of heat flux.

Acknowledgement

The support of this work by the National Science Council of the Republic of China under the Contract No. NSC 95-2221-E-269-025 is gratefully acknowledged.

References

[1] J.V. Beck, B. Blackwell, C.R.St. Clair Jr., Inverse Heat Conduction: Ill-posed Problems, Wiley, New York, 1985.
[2] O.M. Alifanov, Inverse Heat Transfer Problems, Springer-Verlag, New York, 1994.
[3] K. Kurpisz, A.J. Nowak, Inverse Thermal Problems, Computational Mechanics Publications, Southampton, 1995.
[4] M.N. Ozisik, H.R.B. Orlande, Inverse Heat Transfer, Taylor & Francis, New York, 2000.
[5] A. Moutsoglou, Solution of an elliptic inverse convection problem using a whole domain regularization technique, AIAA J. Thermophys. Heat Transfer 4 (3) (1990) 341–349.
[6] M.J. Colaco, H.R.B. Orlande, Inverse forced convection problem of simultaneous estimation of two boundary heat fluxes in irregularly shaped channels, Numer. Heat Transfer Part A: Appl. 39 (7) (2001) 737–760.
[7] C.H. Huang, M.N. Ozisik, Inverse problem of determining unknown wall heat flux in laminar flow through a parallel plate duct, Numer. Heat Transfer Part A: Appl. 21 (1) (1992) 55–70.
[8] F.B. Liu, M.N. Ozisik, Inverse analysis of transient turbulent forced convection inside parallel-plate ducts, Int. J. Heat Mass Transfer 39 (12) (1996) 2615–2618.
[9] R. Raghunath, Determining entrance conditions from downstream measurements, Int. Commun. Heat Mass Transfer 20 (1993) 173–183.
[10] J.C. Bokar, M.N. Ozisik, An inverse analysis for estimating the time-varying inlet temperature in laminar flow inside a parallel plate duct, Int. J. Heat Mass Transfer 38 (1995) 39–45.
[11] F.B. Liu, M.N. Ozisik, Estimation of inlet temperature profile in laminar duct flow, Inverse Probl. Eng. 3 (1996) 131–143.
[12] H.A. Machado, H.R.B. Orlande, Inverse analysis for estimating the timewise and spacewise variation of the heat flux in a parallel plate channel, Int. J. Numer. Math. Heat Fluid Flow 7 (1997) 696–710.
[13] H.M. Park, J.H. Lee, A method of solving inverse convection problem by means of mode reduction, Chem. Eng. Sci. 53 (1998) 1731–1744.
[14] A. Fic, A study of the steady-state inverse heat transfer problem of estimating the boundary velocity, Numer. Heat Transfer Part A: Appl. 45 (2) (2004) 153–170.
[15] H.Y. Li, W.M. Yan, Estimation of space and time dependent wall heat flux in an inverse convection problem, AIAA J. Thermophys. Heat Transfer 13 (3) (1999) 394–396.
[16] H.Y. Li, W.M. Yan, Identification of wall heat flux for turbulent forced convection by inverse analysis, Int. J. Heat Mass Transfer 46 (2003) 1041–1048.
[17] H.Y. Li, W.M. Yan, Inverse convection problem for determining wall heat flux in annular duct flow, ASME J. Heat Transfer 122 (3) (2000) 460–464.
[18] C.K. Chen, L.W. Wu, Y.T. Yang, Comparison of whole-domain and sequential algorithms for function specification method in the inverse heat transfer problem of laminar convective pipe flow, Numer. Heat Transfer Part A: Appl. 50 (10) (2006) 927–947.
[19] W.M. Yan, Y.L. Tsay, T.F. Lin, Transient conjugated heat transfer in laminar pipe flows, Int. J. Heat Mass Transfer 32 (1989) 775–777.
[20] S.V. Patankar, Numerical Heat Transfer and Fluid Flow, Hemisphere, Washington, DC, 1980.
[21] M.R. Hestenes, Conjugate Direction Methods in Optimization, Springer-Verlag, New York, 1980 (Chapter 4).
[22] O.M. Alifanov, Solution of an inverse problem of heat conduction by iteration methods, J. Eng. Phys. 26 (4) (1974) 471–476.
[23] User's Manual: Math Library Version 1.0, IMSL Library Edition 10.0, IMSL, Houston, TX, 1987.